Quantum Chemical Evaluation of Protein Control over Heme Ligation: CO/O_2 Discrimination in Myoglobin

Filippo De Angelis,[‡] Andrzej A. Jarzęcki,[†] Roberto Car, and Thomas G. Spiro*

Chemistry Department, Princeton University, Princeton, New Jersey 08544

Received: October 21, 2004

Control of O_2 versus CO binding in myoglobin (Mb) is tuned by a distal histidine residue through steric and H-bonding interactions. These interactions have been evaluated via Car−Parrinello DFT calculations, whose efficiency allows full quantum mechanical treatment of the 13 closest residues surrounding the heme. The small (8°) deviation of the Fe−C−O bond angle from linearity results from the steric influence of a distal valine residue and not the distal histidine. H-bond energies were evaluated by replacing the distal histidine with the non-H-bonding residue isoleucine. Binding energies for CO and O_2 decreased by 0.8 and 4.1 kcal/mol for MbCO and MbO_2, in good agreement with experimental H-bond estimates. Ligand discrimination is dominated by distal histidine H-bonding, which is also found to stabilize a metastable side-on isomer of MbO_2 that may play a key role in MbO_2 photodynamics.

Introduction

Heme proteins play a unique role in biology as sensors, activators, and carriers of the gaseous molecules O_2, NO, and CO.[1] These XO molecules play vital roles in bioenergetics and in signaling, but being nonpolar or nearly so, are difficult to capture. Nature has harnessed the heme group for this purpose. The d electrons of the heme Fe[II] ion are well-matched to the XO π^* acceptor orbitals allowing for a strong but reversible back-bonding interaction. This fundamental binding mechanism is modulated by noncovalent interactions of the heme−XO complex with the surrounding protein, accounting for wide variations in binding affinity, selectivity, and reactivity. Understanding these interactions is of fundamental importance for elucidating the biological activities of heme proteins.

One of the most celebrated issues in this arena is the nature of the discrimination against CO binding and/or in favor of O_2 binding by hemoglobin (Hb) and myoglobin (Mb), the physiological oxygen carriers of blood and muscle. The natural affinity of heme is some 20 000 times higher for CO than for O_2, but this ratio is reduced about 1000-fold in the proteins,[2] corresponding to a discrimination energy of ∼4 kcal/ mol. How this discrimination is achieved has been a matter of enduring controversy (see citations in ref 3). Two candidate explanations have been proposed: (i) steric hindrance to CO binding[4] and (ii) H-bond stabilization of bound O_2, relative to bound CO.[5]

Both explanations focus on a distal histidine residue, which is positioned over the heme Fe in both Mb and Hb (see Figure 1),[6,7] where it can interact with bound ligands. The steric explanation recognizes that the FeCO unit is naturally linear, while the FeO_2 unit is naturally bent, for electronic reasons; the two additional electrons of O_2 with respect to CO populate an antibonding π^* orbital, which is empty in the CO case. Thus, the distal histidine might inhibit CO binding sterically, by forcing the naturally linear FeCO unit to assume a partially bent geometry, whereas O_2 binding would be unaffected. On the other hand, the H-bonding explanation depends on the distal histidine side chain having a moderately acidic NH group. It can H-bond more favorably with bound O_2 than with bound CO because of the greater negative charge on O_2, where π^* orbitals are lower in energy and attract the Fe d electrons more strongly than CO.

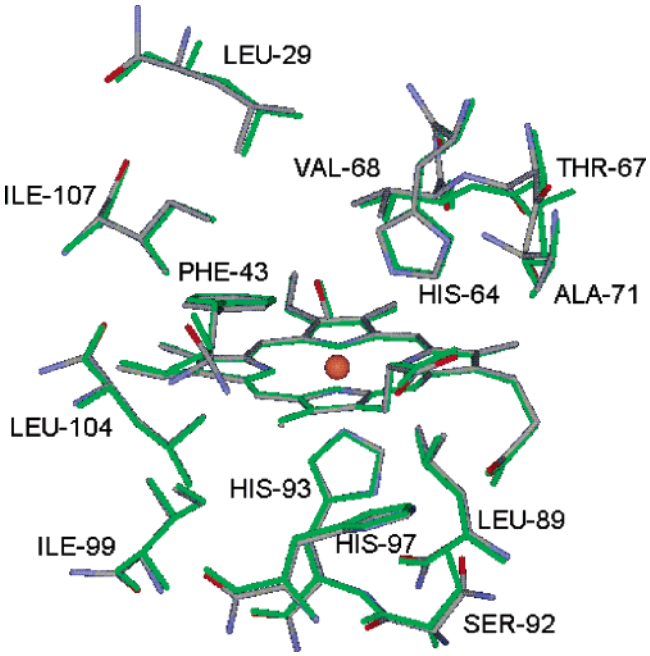

Figure 1. Overlay of residues and heme positions for the Mb(His64)-CO model calculation (gray) and X-ray (ref 10) coordinates (green).

The steric hindrance idea gained plausibility from early MbCO crystal structures, both X-ray[6] and neutron,[7] whose electron density was modeled with decidedly bent, albeit disordered, CO ligands. However, later X-ray structures revealed much less bending,[8−11] and it seems likely, in retrospect, that the early structures were affected by oxidation to met-Mb in the course of lengthy data collection (met-Mb would have a

* Corresponding author. E-mail: spiro@princeton.edu.
† Present address: Chemistry Department, Brooklyn College of the City University of New York, Brooklyn, NY 11210.
‡ Present address: Istituto CNR di Scienze e Tecnologie Molecolari (ISTM), Dipartimento di Chimica, Universitá di Perugia, Via Elce di Sotto 8, I-06123, Perugia, Italy.

10.1021/jp0451851 CCC: $30.25
Published on Web 02/02/2005

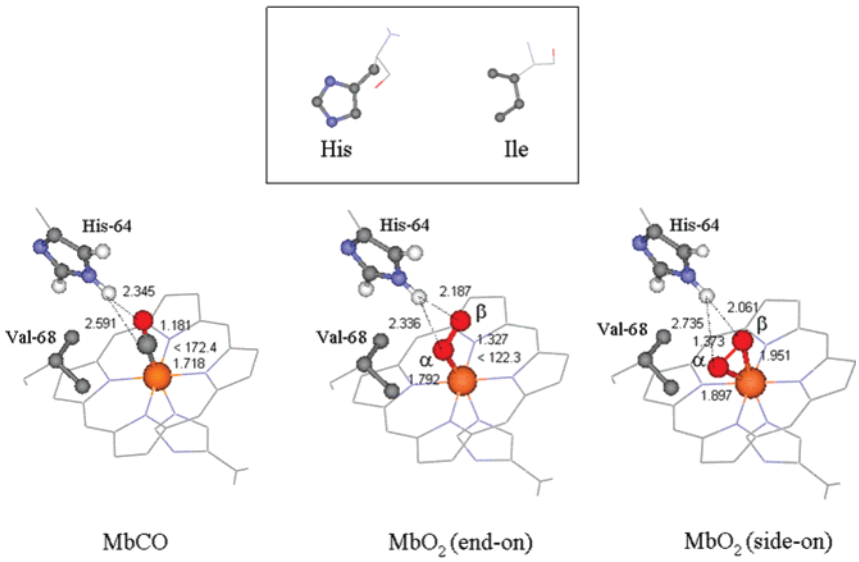

Figure 2. Computed ligand positions and geometric parameters for MbCO and for MbO_2 in both end-on and side-on (metastable) configurations.

water molecule bound to Fe(III) instead of CO bound to Fe(II)[8]). In agreement with this hypothesis, model calculations using DFT have indicated that the energy requirement for the modest distortions seen in recent MbCO crystal structures is small, <1 kcal/mol.[12−15]

Nevertheless, the CO geometry alone is not decisive since energy might be stored in displacements of the protein. In an earlier examination of this question,[3] we used equilibrium and kinetic binding data from Olson and co-workers[2] on Mb variants having hydrophobic residues in place of the distal histidine. These variants lose most of the ∼4 kcal discrimination energy and establish the key role of the distal histidine. However, the analysis indicated that H-bonding accounted for almost all (∼85%) of the effect. Thus, the distal histidine appears to offer little steric hindrance to CO binding. This conclusion is supported by crystallographic evidence that the distal histidine side chain is rather flexible in MbCO, as indicated by high temperature factors[11] or significant population of alternative conformations[10] and also by molecular dynamics simulations indicating little resistance to side chain rotation.[16,17]

Since our analysis of the experimental data rested on several assumptions,[3] it seemed worthwhile to test the results computationally. In the present study, we have carried out DFT calculations on MbCO and MbO_2, using the Car−Parrinello method[18] to model the effects of the surrounding protein on the heme adducts. The wild-type protein was compared with a variant, His64Ile, in which the distal histidine was replaced by isoleucine (see Figure 2). Ile is representative of the hydrophobic but nearly isosteric replacements, Ile, Leu and Val, for which data are available;[2,3] having a residue of nearly the same size as histidine is important to avoid additional steric effects, or else incursion of water molecules into the cavity formed when smaller residues (Ala, Gly) are substituted.[2]

DFT has previously been used to explore structure and bonding in complexes modeling the XO adducts of heme,[12−15,19−31] and the issue of H-bonding has been explored with H-bond donors placed at various positions distal to the bound XO.[32−35] In addition, the heme−XO adduct has been embedded in Mb, and the system was treated by QM/MM (quantum mechanics/molecular mechanics) methods.[23,36] However, the present study is the first one to treat a full complement of residues packed around the heme−XO complex at a fully quantum mechanical level. Gratifyingly, the results reproduce experimental structures and energies with good accuracy and illuminate the mechanism of ligand discrimination. In addition, the computations reveal a metastable side-on structure for MbO_2, which seems to play an important role in MbO_2 photodynamics.

Materials and Methods

The heme site model of Mb (Figure 1) was based on a high-resolution crystal structure of MbCO (pdb code: 1BZR).[10] Thirteen residues were retained, which had atoms falling within a 8 Å radius of the Fe atom. Six of these were on the proximal side—Leu 89, Ser 92, His 93, His 97, Ile 99, and Leu 104—and seven were on the distal side of the heme—Leu 29, Phe 43, His 64, Thr 67, Val 68, Ala 71, and Ile 107. All residues were terminated with amino groups (NH_2-) and amido groups ($-CO-NH_2$). Two residues, Leu 29 and Leu 104, were randomly chosen to be terminated with an extra hydrogen atom on terminal amido groups ($-CO-NH_3^{+-}$), to neutralize the two negatively charged propionate side chains of the heme. Later, it was determined that ligand binding energies do not show significant variations with respect to the position or even the presence of the two extra protons.

The distal histidine, His 64, was modeled as the N_ϵ tautomer, with the proton directed at the CO ligand (see Figure 2). A variety of evidence strongly favors this tautomer,[34,35,37−40] early neutron diffraction results to the contrary[7] notwithstanding. (Along with the highly bent CO, the N_δ tautomer in the neutron structure probably reflected autoxidation during lengthy data collection, with Fe(II)CO being replaced by $Fe(III)OH_2$[8].) The initial structure of the His64Leu mutant was obtained by replacing the His64 side chain with isoleucine side chain atoms at standard bond distances and angles. To model the MbO_2 heme site, the CO ligand was replaced with O_2 in the same starting structures.

Calculations were performed with the parallel version of the CP code[41] implementing Vanderbilt pseudopotentials[42,43] and the PBE[44] exchange−correlation (XC) functional. Core states were projected out using pseudopotentials; for all the atomic species, ultra-soft pseudopotentials were generated according to the scheme proposed by Vanderbilt.[45] The wave functions were expanded in plane waves up to an energy cutoff of 25 Ry, while a 200 Ry cutoff was used for expansion of the augmented charge density. Periodic boundary conditions (PBC) were used by placing the molecules in a cubic box of 25.04 Å,

keeping a minimum of 5.0 Å between repeated images, sufficiently large to avoid any coupling between periodic images. Corrections to the electrostatic energy of a charged system in PBC were added, as needed.[19] We recognize that the nonhybrid XC functional would be less successful than hybrid functionals (which include some amount of Hartree−Fock exchange) for puposes of computing ligand-binding energies. We have not attempted to compute these quantities, restricting ourselves to the evaluation of contributions from H-bonding and steric effects. Nonhybrid XC functionals have proven to be reliable in predicting energies and structural parameters of hydrogen-bonding interaction systems, including the extreme case of the hydrogen-bonding network of liquid water.[46−48]

CP geometry optimizations were performed using an integration time step of 15 au and the same mass for all the ions, 12 amu. For the calculations involving the O_2 ligand, we considered an open shell singlet wave function since this electronic configuration has been shown to correspond to the ground state for O_2−iron porphyrin complexes.[15] Overall, the wild-type and His64Ile models consisted of 336 and 340 atoms, respectively, and a maximum of 902 electrons; this probably represents the largest full quantum mechanical calculation ever attempted on a heme protein. This should be regarded as a benchmark study. It is possible that some of the residues, or parts of them, could have been omitted without seriously affecting the results. We have not investigated this issue systematically, although partial calculations for the purpose of examining steric effects are described next.

Structures were fully optimized, without any symmetry constraints, using damped nuclear and electronic dynamics, alternating with free molecular dynamics, to achieve the most efficient sampling of the potential energy surface. The terminal amino nitrogen atoms were initially frozen at the positions they occupy in the crystal structure; subsequently, these constraints were removed allowing all degrees of freedom to fully relax. Similar optimization was performed on imidazole-bound Fe(II)porphine complexes ([ImH]FePL; L= CO, O_2) as reference structures. In addition, limited calculations were carried out on the MbCO model with only specific residues included (see next).

All the calculations have been performed on a SGI Origin computer with 64 × 300 MHz MIPS12000 processors. A typical geometry optimization run of the largest 336 and 340 atoms systems involves about 500 time-steps, for a total CPU wall-time using 16 processors of about 10 days and an overall memory usage close to 8 Gb. Such large-scale DFT calculations have been possible due to the inherent computational efficiency of the Car−Parrinello algorithm implementing Vanderbilt pseudo-potentials[42,43] and to the effective parallel implementation of this algorithm that has been recently achieved.[19]

Results and Discussion

MbCO Structure: Source of CO Distortion. Figure 1 compares the optimized model structure with the starting crystal structure of MbCO. The structures are nearly indistinguishable, with rms deviation of 0.13 Å for the heavy (non-hydrogen) atoms. Thus, the modeled heme site is quantum mechanically stable, despite the absence of the surrounding protein. Notably, for the atoms of the heme-CO complex alone, the rms deviation from the MbCO structure is only 0.02 Å.

Critical interatomic distances are compared in Table 1. In agreement with previous DFT results,[21,24,32] the [ImH]FeP[CO] parameters are in excellent agreement with the crystal structure[49] of [Py]FeTPP[CO] (TPP = tetraphenylporphine and Py = pyridine), except for a slightly longer C−O bond. This small discrepancy may be attributable to the XC functional used in the calculation since a slightly shorter distance (1.15 Å) has been computed with the hybrid B3LYP functional.[50,51] The agreement between model and X-ray MbCO parameters is almost as good and is probably within the uncertainty of the X-ray parameters. The His64 N_ϵ atom is calculated to be 3.09 Å from the O atom of the bound CO, close to the 3.21 Å experimental value, and consistent with a weak H-bond, as suggested by the small shift of the C−O stretching frequency upon H/D exchange.[37] The distal histidine interacts with the bound CO in a sideways fashion (Figure 2), forming an <O−H−N_ϵ angle of 126°; this result supports Franzen's theoretical analysis[33] showing a preferential sideways interaction between bound CO and H-bond donors in iron−porphyrin complexes. When His64 is replaced by Ile, eliminating the H-bonding, the computed Fe−C distance increases by 0.010 Å, while the C−O distance decreases by 0.005 Å. These compensating changes reflect the importance of back-bonding in the FeCO unit, and the role of positive polarity distal to the CO in enhancing back-bonding, as has been deduced from spectroscopic and computational studies.[20]

TABLE 1: Computational and Experimental Structure Parameters (Å, Degree) for MbCO and a Model Complex

				(L)Fe^{II}P(CO)	
	MbCO			P = porphyrin	P = TPP
	WT Mb		H64I	L = ImH	L = pyridine
	expt.[10]	calcd	calcd	calcd	expt.[49]
CO−N_ϵ	3.21	3.09			
CO−NH_ϵ		2.35			
C−O	1.13	1.18	1.18	1.179	1.12(2)
Fe−C	1.73	1.72	1.73	1.725	1.77(2)
Fe−$N_{p(av)}$	2.01	2.02	2.02	2.012	2.015
Fe−N_{prox}	2.11	2.10	2.11	2.112	2.10(1)
<Fe−C−O	171.3	172.4	172.4	179.3	179(2)

In the absence of constraining factors, the Fe−C−O bonds are expected to be collinear, and indeed, both experimental and computational studies give a <FeCO = 179° for the protein-free models. In MbCO, the angle decreases to 171°, and this parameter is very well-reproduced (172°) by the present computation. Strikingly, however, the angle does not change at all in the computed heme site of the His64Ile variant (see Table 1). Thus, the FeCO distortion from linearity is not due to interaction with the distal histidine side chain. (The other distortion coordinate, Fe−C tilting from the normal to the heme plane, is negligible, <2°, in the crystal structure and in computational structures.)

Indeed, examination of the MbCO optimized structure shows that the Fe−C−O unit bends away from another distal residue, Val68 (Figure 2). Consequently, we compared the effects of Val68 and His64, in limited computations that included the heme group and the proximal histidine ligand (His 93), and Val68 and/or His 64 or neither. In these calculations, all atoms were frozen at their optimized positions in the full MbCO model, except for the FeCO unit, which was allowed to relax. Without any distal residues <FeCO was 180°, but inclusion of Val68 reduced <FeCO to 173°, close to its value in the full MbCO model. Adding His64 had almost no effect on these values; <FeCO is 177° when His64 was the only distal residue and 171° when both Val68 and His64 were present. Thus, we can confidently conclude that the 8° distortion of FeCO from linearity, observed in MbCO, is essentially due to steric hindrance from Val68.

TABLE 2: Computed and Experimental Structure Parameters (Å, Degree) for MbO_2 and a Model Complex

	MbO_2			$(IMH)Fe^{II}P(O_2)$	
	WT		H64I	P = porphine	P-TivP
	expt.[11]	calcd	calcd	calcd	expt.[52]
$O_\alpha-N_\epsilon$	3.08	3.26			
$O_\beta-N_\epsilon$	2.97	3.06			
$O_\alpha-HN_\epsilon$		2.34			
$O_\beta-HN_\epsilon$		2.19			
O−O	1.24	1.33	1.30	1.152	1.16(8)
$Fe-O_\alpha$	1.81	1.79	1.80	1.788	1.75(2)
$Fe-N_{p(av.)}$	2.01	2.01	2.01	2.023	1.996(4)
$Fe-N_{prox}$	2.01	2.09	2.09	2.077	2.07(2)
$Fe-O_\alpha-O_\beta$	122.5	122.3	124.2	122.4	131

We note that Kachalova et al.[10] have proposed on the basis of high-resolution MbCO and deoxyMb crystal structures that steric hindrance from Val68 is responsible for the ability of Mb to discriminate against CO, relative to O_2. They observed that Val68 is even closer to the heme Fe in deoxyMb and is shifted away upon binding CO. Indeed, the measured CO binding energy does increase when Val68 is replaced by a smaller residue, alanine,[2] but the effect is only 0.4 kcal/mol, much less than the ∼4 kcal/mol discrimination energy.

The absence of any influence of the FeCO geometry when His64 is added or removed from the model lends strong support to the view that the distal histidine side chain offers no significant steric inhibition to CO binding.[10,11,16,17]

MbO_2 Structure: End-On versus Side-On Binding. To model MbO_2, we replaced CO with O_2 in the MbCO structure and reoptimized the 336 atom fragment. Outside the FeO_2 unit and the distal histidine, atomic displacements were minimal, consistent with an otherwise unperturbed heme site; the rms deviation, relative to the MbO_2 crystal structure, was 0.17 Å for the 336 atoms and 0.02 Å for the atoms of the heme−O_2 complex.

Interatomic distances (Table 2) are again in good agreement with X-ray structures. [ImH]FeP[O_2] parameters are close to those measured for a picket fence porphyrin complex[52] (the pickets prevent intermolecular reaction to produce the stable μ-oxo dimer). Likewise, the distances agree well between the MbO_2 model and the crystal structure; the Fe−O−O angle is close to 122° in both. The distal His64 side chain moves slightly closer to the bound ligand than in MbCO, and the H-bond to the terminal O atom is shortened (2.19 Å); a moderately strong H-bond is also experienced by the inner O atom (2.34 Å). Despite the importance of these H-bonds to the binding energy (see next), replacement of His64 by Ile has almost no effect on the FeO_2 geometry, except that the Fe−O distance is increased by 0.006 Å while the O−O distance is decreased by 0.010 Å. These compensating changes attest to the importance of back-bonding in FeO_2, as well as FeCO adducts, as has been inferred from vibrational spectroscopy.[21]

Further computations, in which the Fe−O−O angle was systematically varied, led us to the discovery of a metastable structure, in which the O_2 is bound sideways, with bonds from Fe to both O atoms, as illustrated in Figure 2. The Fe−O (1.90−1.95 Å) and O−O (1.37 Å) distances are single bond distances, and indeed, the structure resembles those of known side-on Fe(III) peroxides.[53−55] However, electron counting requires an Fe(IV) peroxide formulation since peroxide has two more electrons than O_2. The stable end-on structure can be formulated as Fe(III) superoxide;[56] the short O−O distance, 1.33 Å, is characteristic of the superoxide ion. Indeed, we found the computed Mulliken charges on the O_2 moiety to increase from −0.32 to −0.48, between the end-on and the side-on structure.

The computed energy is 10.7 kcal/mol higher for the side-on than the end-on isomer, but the former does exist in a local minimum, relative to changes in the Fe−O−O angle. It is interesting to notice that in absence of the protein environment (i.e., when [ImH]FeP[O_2] is computed), the energy difference between the two isomers increases to 16.9 kcal/mol. Thus, the side-on isomer is stabilized by the protein pocket polarity and by H-bonds from the His64 side chain (Figure 2), reflecting the importance of the increased negative charge on the bound O_2. We note that the energetics of side-on versus end-on O_2 binding to a model heme was earlier explored via semiempirical INDO calculations.[57]

To check on the adequacy of our nonhybrid functional in this application, we performed single-point calculations on [ImH]FeP[O_2] with the B3LYP hybrid functional, as implemented in the Gaussian 03 program[58] package at the CP-PBE optimized geometry. Two basis sets, LANL2DZ[59] and 6-3111G*,[60,61] gave energy differences of 18.2 and 17.2 kcal/mol between the side-on and end-on isomers. These values are in accord with the 16.9 kcal/mol CP-BPE energy difference and establish that the isomerization energy is insensitive to the choice of hybrid versus nonhybrid functionals. Of course, the energy is highly dependent on geometry, and when the geometry is allowed to optimize within the B3LYP/LANL2DZ potential, the energy difference between the isomers diminishes to 11.5 kcal/mol, a value already reported.[62] This large relaxation effect probably results from inclusion of 20% Hartree−Fock exhange in the hybrid functional, which favors ionic configurations; as noted previously, charge transfer from Fe to O_2 increases for the side-on isomer. The point remains that the protein lowers the energy difference in the CP-PBE computation because of the polarity of the binding pocket.

There is experimental evidence that the side-on isomer can be trapped at low temperature upon photoexcitation of an Fe(II)porphyrin−O_2 adduct.[63] Moreover, MbO_2 at low temperature shows a sizable nonphotolyzable fraction, which has been suggested to arise from isomerization to the side-on structure.[64,65] Motivated by this evidence, we recently examined the heme−O_2 excited states computationally[62] and showed that the side-on isomer provides a facile path for return to the ground state after photoexcitation, thereby explaining the low photodissociation quantum yield of MbO_2. Thus, the side-on isomer may play an important role in the photodynamics of heme-bound O_2. We note that side-on bound O_2 has been characterized crystallographically in a non-heme iron protein.[66]

Energetics and Ligand Discrimination. To evaluate the interaction energy of the distal histidine with the bound ligand, we computed the energy difference between the wild-type and His64Ile heme site models and subtracted the energy difference between the isolated histidine and isoleucine residues. The resulting values are 0.83 and 4.08 kcal/mol for MbCO and MbO_2, respectively; they represent the effect of substituting the distal histidine with isoleucine. The computations do not include enthropy effects, but these are expected to be small for substituting one residue with another.

The computed interaction energies are compared in Table 3 with two sets of estimates deriving from experimental data.[3] One is the quantity ΔE_L, calculated from the measured ligand dissociation rate constants:[2] $\Delta E_L = kT\Delta\ln k_{diss}$, where the Δ refers to the difference between the wild-type and His64Ile variants of Mb. The assumption is that ligand dissociation, being an elementary process, is a direct measure of the Fe−ligand

TABLE 3: Energy Diference (kcal/mol) for the His64Ile Substitution in MbCO and MbO_2

		experimental	
ligand	computed	ΔE_L[a]	$\Delta\Delta G_{corr}$[b]
CO	0.83	0.54	0.03
O_2	4.08	3.58	3.58
$\Delta[\Delta O_2-CO]$	3.25	3.04	3.55

[a] $\Delta E_L = kT\Delta k_L$, k_L = dissociation rate constant for CO and O_2. [b] $\Delta\Delta G_{coor}$ binding free energy difference, corrected for the estimated free energy for binding a water molecule to deoxyMb, 1.12 kcal/mol.

bond strength, as modulated by distal interactions. The ΔE_L values are remarkably close to the computed interaction energies; the former are 0.3−0.4 kcal/mol lower than the latter, certainly within the uncertainties of both sets of estimates. This agreement indicates that the effect of H-bonding on the Fe−ligand bond strength is properly captured by the computation and validates ΔE_L as a measure of the bond strength change.

Another relevant experimental quantity is the difference between the binding free energies for wild-type and His64Ile variants, $\Delta\Delta G_L$, based on the equilibrium binding constants. $\Delta\Delta G_L = 2.46$ and -1.09 kcal/mol for O_2 and CO.[2,3] However, these quantities must be corrected for the deoxyMb energy difference, ΔE_{dx}, between the two variants, mainly reflecting the presence of a water molecule H-bonded to the distal histidine in wild-type deoxyMb, which is missing in the His64Ile variant.[67] This energy was estimated to be -1.12 kcal/mol, by assuming that $\Delta\Delta G_L = \Delta E_L + \Delta E_{dx}$ in the case of O_2 binding. When this value is used as a correction, $\Delta\Delta G_L^{corr} = \Delta\Delta G_L + 1.12 = 3.58$ kcal/mol for O_2 ($= \Delta E_L$) and 0.03 kcal/mol for CO (Table 3). The 0.51 kcal/mol difference between $\Delta\Delta G_L^{corr}$ and ΔE_L for MbCO was attributed to the steric effect of His64 on CO binding, which would not appear in the altered Fe−CO bond strength.[3] In this view, the essentially zero value for $\Delta\Delta G_L^{corr}$ of MbCO results from the cancellation of a favorable H-bond interaction and an unfavorable steric interaction, both worth ∼0.5 kcal/mol.

The computed energy difference should encompass both electronic and steric effects, and the proper reference value should therefore be $\Delta\Delta G_L^{corr}$. However, as noted previously, the computed geometries suggest that the steric effect of His64 is negligible, and the computed energy difference for MbCO is indeed close to ΔE_L. It is possible that the computation cannot capture a steric effect as small as 0.5 kcal/ mol; it is also possible that experimental uncertainties exceed 0.5 kcal/mol. In any event, the steric effect is clearly very small. The influence of His64, which accounts for most of the CO versus O_2 discrimination, is essentially a differential H-bond effect. The His64 contribution to the discrimination energy, as measured by the O_2/CO energy difference upon His/Ile substitution, is computed to be 3.25 kcal/mol, midway between the ΔE_L and $\Delta\Delta G_L^{corr}$ differences (Table 3).

This differential H-bonding has previously been examined computationally in simpler models. Computing H-bond energies for imidazole interacting with a ligated heme model, via DFT and the counterpoise method, Sigfridsson and Ryde obtained 1.9 and 7.6 kcal/mol for the CO and O_2 adducts.[33] More recently, they carried out QM/MM calculations on MbO_2 and MbCO, treating the heme adduct quantum mechanically and the protein via molecular mechanics.[36] The computed H-bond energy diminished to 0.5−0.7 kcal/mol for CO, in agreement with the present value, but remained high, 6.7−7.2 kcal/mol for O_2.[36] In another recent QM/MM computation of the same proteins, Rovira et al.[23] obtained H-bond energies of 3.3 and 5.0 kcal/mol for the CO and O_2 adducts. Thus, the estimates depend in detail on the computational method. The present results indicate that full quantum treatment of the heme site gives values that are closest to experiment.

Another test is provided by Phillips et al.'s[39] finding that the log of the ligand dissociation rate correlates linearly with the electrostatic potential of the Mb binding pocket, as computed via a linearized Poisson−Boltzmann method; this is the effect expected if the Fe−ligand bond strength is modulated by polarity (e.g., H-bonding) effects. The correlation was obtained for a large number of residue substitutions in the binding pocket, and the slope was four times larger for O_2 than for CO. This behavior is consistent with O_2 being four times as strong a H-bond acceptor as CO, when bound to heme, although the relative H-bond strengths in any particular variant depend on the placement of the pocket residues since the FeCO and FeO_2 geometries differ. The computed H-bond energy ratio is five in the present study and four in Sigfridsson and Ryde's model study,[33] but ∼10 and 1.5 in the two QM/MM protein studies.[22,35]

Conclusions

This study establishes that the Car−Parrinello DFT methodology can successfully model the electronic properties of the heme group and its noncovalent interactions with the surrounding protein. The calculation reproduced the FeCO geometry of MbCO and established that the modest displacement from linearity is attributable to a steric interaction with a valine residue in the binding pocket and not with the distal histidine. The latter interacts by forming H-bonds, weakly with CO and more strongly with O_2. The interaction energies, computed by relplacing the distal histidine with a non H-bonding residue, isoleucine, are in excellent agreement with the experimental estimate from ligand dissociation rates. Differential H-bonding by the distal histidine is clearly the dominant mechanism for ligand discrimination in Mb; the H-bond to bound O_2 is about five times stronger than the H-bond to bound CO. H-bonding from the distal histidine also stabilizes a side-on bound metastable isomer of the O_2 adduct, which may play a critical role in photodynamics.

References and Notes

(1) Spiro, T. G.; Jarzecki, A. A. *Curr. Opin. Chem. Biol.* **2001**, *5*, 715.
(2) Springer, B. A.; Sligar, S. G.; Olson, J. S.; Phillips, G. N., Jr. *Chem. Rev.* **1994**, *94*, 699.
(3) Spiro, T. G.; Kozlowski, P. M. *Acc. Chem. Res.* **2001**, *34*, 137.
(4) Collman, J. P.; Fu, L. *Acc. Chem. Res.* **1999**, *32*, 455.
(5) Momenteau, M.; Reed, C. A. *Chem. Rev.* **1994**, *94*, 659.
(6) Kuriyan, J.; Wilz, S.; Karplus, M.; Petsko, G. A. *J. Mol. Biol.* **1986**, *192*, 133.
(7) Cheng, X. D.; Schoenborn, B. P. *Acta Crystallogr., Sec. B* **1990**, *46*, 195.
(8) Quillin, M. L.; Arduini, R. M.; Olson, J. S.; Phillips, G. N. *J. Mol. Biol.* **1993**, *234*, 140.
(9) Yang, F.; Phillips, G. N. *J. Mol. Biol.* **1996**, *256*, 762.
(10) Kachalova, G. S.; Popov, A. N.; Bartunik, H. D. *Science* **1999**, *284*, 473.
(11) Vojtechovsky, J.; Chu, K.; Berendzen, J.; Sweet, R. M.; Schlichting, I. *Biophys. J.* **1999**, *77*, 2153.
(12) Ghosh, A.; Bocian, D. F. *J. Phys. Chem.* **1996**, *100*, 6363.
(13) Vangberg, T.; Bocian, D. F.; Ghosh, A. *J. Biol. Inorg. Chem.* **1997**, *2*, 526.
(14) Kozlowski, P. M.; Vogel, K. M.; Zgierski, M. Z.; Spiro, T. G. *J. Porphyrin Phthalocyanines* **2001**, *5*, 312.
(15) Rovira, C.; Kunc, K.; Hutter, J.; Ballone, P.; Parrinello, M. *J. Phys. Chem. A* **1997**, *101*, 8914.
(16) Jewsbury, P.; Kitagawa, T. *Biophys. J.* **1994**, *67*, 2236.
(17) Schulze, B. G.; Evanseck, J. D. *J. Am. Chem. Soc.* **1999**, *121*, 6444.
(18) Car, R.; Parrinello, M. *Phys. Rev. Lett.* **1985**, *55*, 2471.
(19) Spiro, T. G.; Kozlowski, P. M. *J. Am. Chem. Soc.* **1998**, *120*, 4524.
(20) Vogel, K. M.; Kozlowski, P. M.; Zgierski, M. Z.; Spiro, T. G. *Inorg. Chim. Acta* **2000**, *297*, 11.

(21) Vogel, K. M.; Kozlowski, P. M.; Zgierski, M. Z.; Spiro, T. G. *J. Am. Chem. Soc.* **1999**, *121*, 9915.
(22) Spiro, T. G.; Zgierski, M. Z.; Kozlowski, P. M. *Coord. Chem. Rev.* **2001**, *219*−*221*, 923.
(23) Rovira, C.; Schulze, B.; Eichinger, M.; Evanseck, J. D.; Parrinello, M. *Biophys. J.* **2001**, *81*, 435.
(24) Franzen, S. *J. Am. Chem. Soc.* **2001**, *123*, 12578.
(25) McMahon, M. T.; deDios, A. C.; Godbout, N.; Salzmann, R.; Laws, D. D.; Le, H. B.; Havlin, R. H.; Oldfield, E. *J. Am. Chem. Soc.* **1998**, *120*, 4784.
(26) Zhang, Y.; Gossman, W.; Oldfield, E. *J. Am. Chem. Soc.* **2003**, *125*, 16387.
(27) Ghosh, A.; Wondimagegn, T. *J. Am. Chem. Soc.* **2000**, *122*, 8101.
(28) Conradie, J.; Wondimagegn, T.; Ghosh, A. *J. Am. Chem. Soc.* **2003**, *125*, 4968.
(29) Barea, G.; Maseras, F.; Lledos, A. *Intl. J. Quant. Chem.* **2001**, *85*, 100.
(30) Marechal, J.-D.; Maseras, F.; Lledos, A.; Mouaward, L.; Perahia, D. *Chem. Phys. Lett.* **2002**, *353*, 379.
(31) Wondimagegn, T.; Ghosh, A. *J. Am. Chem. Soc.* **2001**, *123*, 5680.
(32) Sigfridsson, E.; Ryde, U. *J. Biol. Inorg. Chem.* **1999**, *4*, 99.
(33) Franzen, S. *J. Am. Chem. Soc.* **2002**, *124*, 13271.
(34) Kushkuley, B.; Stavrov, S. S. *Biophys. J.* **1996**, *70*, 1214.
(35) Kushkuley, B.; Stavrov, S. S. *Biophys. J.* **1997**, *72*, 899.
(36) Sigfridsson, E.; Ryde, U. *J. Inorg. Biochem.* **2002**, *91*, 101.
(37) Unno, M.; Christian, J. F.; Olson, J. S.; Sage, J. T.; Champion, P. M. *J. Am. Chem. Soc.* **1998**, *120*, 2670.
(38) Straub, J. E.; Karplus, M. *Chem. Phys.* **1991**, *158*, 221.
(39) Phillips, G. N.; Teodoro, M. L.; Li, T. S.; Smith, B.; Olson, J. S. *J.Phys. Chem. B* **1999**, *103*, 8817.
(40) Cui, Q.; Karplus, M. *J. Chem. Phys.* **2000**, *112*, 1133.
(41) Giannozzi, P.; De Angelis, F.; Car, R. *J. Chem. Phys.* **2004**, *120*, 5903.
(42) Pasquarello, A.; Laasonen, K.; Car, R.; Lee, C. Y.; Vanderbilt, D. *Phys. Rev. Lett.* **1992**, *69*, 1982.
(43) Laasonen, K.; Pasquarello, A.; Car, R.; Lee, C.; Vanderblit, D. *Phys. Rev. B* **1993**, *47*, 10142.
(44) Perdew, J. P.; Burke, K.; Ernzerhof, M. *Phys. Rev. Lett.* **1996**, *77*, 3865.
(45) Vanderbilt, D. *Phys. Rev. B* **1990**, *41*, 7892.
(46) Silvestrelli, P. L.; Parrinello, M. *J. Chem. Phys.* **1999**, *111*, 3572.
(47) Silvestrelli, P. L.; Parrinello, M. *Phys. Rev. Lett.* **1999**, *82*, 3308.
(48) Hetenyi, B.; De Angelis, F.; Giannozzi, P.; Car, R. *J. Chem. Phys.* **2004**, *120*, 8632.
(49) Peng, S. M.; Ibers, J. A. *J. Am. Chem. Soc.* **1976**, *98*, 8032.
(50) Becke, A. D. *J. Chem. Phys.* **1993**, *98*, 1372.
(51) Becke, A. D. *J. Chem. Phys.* **1993**, *98*, 5648.
(52) Jameson, G. B.; Rodley, G. A.; Robinson, W. T.; Gagne, R. R.; Reed, C. A.; Collman, J. P. *Inorg. Chem.* **1978**, *17*, 850.
(53) Neese, F.; Solomon, E. I. *J. Am. Chem. Soc.* **1998**, *120*, 12829.
(54) Rohde, J.-U.; Bukowski, M. R.; Que, L. J. *Curr. Opin. Chem. Biol.* **2003**, *7*, 674.
(55) Friesner, R. A.; Baik, M.-H.; Gherman, B. F.; Guallar, V.; Wirstam, M.; Murphy, R. B.; Lippard, S. J. *Coord. Chem. Rev.* **2003**, *238*−*239*, 267.
(56) Weiss, J. J. *Nature* **1964**, *202*, 83.
(57) Bertran, J.; Ruizlopez, M. F.; Rinaldi, D. *THEOCHEM* **1991**, *78*, 337.
(58) Frisch, M. J.; Trucks, G. W.; Schlegel, H. B.; Scuseria, G. E.; Robb, M. A.; Cheeseman, J. R.; Montgomery, J. A., Jr.; Vreven, T.; Kudin, K. N.; Burant, J. C.; Millam, J. M.; Iyengar, S. S.; Tomasi, J.; Barone, V.; Mennucci, B.; Cossi, M.; Scalmani, G.; Rega, N.; Petersson, G. A.; Nakatsuji, H.; Hada, M.; Ehara, M.; Toyota, K.; Fukuda, R.; Hasegawa, J.; Ishida, M.; Nakajima, T.; Honda, Y.; Kitao, O.; Nakai, H.; Klene, M.; Li, X.; Knox, J. E.; Hratchian, H. P.; Cross, J. B.; Adamo, C.; Jaramillo, J.; Gomperts, R.; Stratmann, R. E.; Yazyev, O.; Austin, A. J.; Cammi, R.; Pomelli, C.; Ochterski, J. W.; Ayala, P. Y.; Morokuma, K.; Voth, G. A.; Salvador, P.; Dannenberg, J. J.; Zakrzewski, V. G.; Dapprich, S.; Daniels, A. D.; Strain, M. C.; Farkas, O.; Malick, D. K.; Rabuck, A. D.; Raghavachari, K.; Foresman, J. B.; Ortiz, J. V.; Cui, Q.; Baboul, A. G.; Clifford, S.; Cioslowski, J.; Stefanov, B. B.; Liu, G.; Liashenko, A.; Piskorz, P.; Komaromi, I.; Martin, R. L.; Fox, D. J.; Keith, T.; Al-Laham, M. A.; Peng, C. Y.; Nanayakkara, A.; Challacombe, M.; Gill, P. M. W.; Johnson, B. G.; Chen, W.; Wong, M. W.; Gonzalez, C.; Pople, J. A. Gaussian 03. Revision B.04; Gaussian, Inc: Pittsburgh, PA, 2003.
(59) Hay, P. J.; Wadt, W. R. *J. Chem. Phys.* **1985**, *82*, 270.
(60) Watchers, A. J. H. *J. Chem. Phys.* **1970**, *52*, 1033.
(61) Hay, P. J. *J. Chem. Phys.* **1977**, *66*, 4377.
(62) De Angelis, F.; Car, R.; Spiro, T. G. *J. Am. Chem. Soc.* **2003**, *125*, 15710.
(63) Watanabe, T.; Ama, T.; Nakamoto, K. *J. Phys. Chem.* **1984**, *88*, 440.
(64) Chance, M. R.; Courtney, S. H.; Chavez, M. D.; Ondrias, M. R.; Friedman, J. M. *Biochemistry* **1990**, *29*, 5537.
(65) Miller, L. M.; Patel, M.; Chance, M. R. *J. Am. Chem. Soc.* **1996**, *118*, 4511.
(66) Karlsson, A.; Parales, J. V.; Parales, R. E.; Gibson, D. T.; Eklund, H.; Ramaswamy, S. *Science* **2003**, *299*, 1039.
(67) Olson, J. S.; Phillips, G. N. *J. Biol. Inorg. Chem.* **1997**, *2*, 544.